

## Photoluminescence characteristics of polar and nonpolar AlGaN/GaN superlattices

Z. Vashaei, C. Bayram, P. Lavenus, and M. Razeghi<sup>a)</sup>

*Center for Quantum Devices, Department of Electrical Engineering and Computer Science, Northwestern University, Evanston, Illinois 60208, USA*

(Received 11 August 2010; accepted 2 September 2010; published online 23 September 2010)

High quality  $\text{Al}_{0.2}\text{Ga}_{0.8}\text{N}/\text{GaN}$  superlattices (SLs) with various (GaN) well widths (1.6 to 6.4 nm) have been grown on polar c-plane and nonpolar m-plane freestanding GaN substrates by metal-organic chemical vapor deposition. Atomic force microscopy, high resolution x-ray diffraction, and photoluminescence (PL) studies of SLs have been carried out to determine and correlate effects of well width and polarization field on the room-temperature PL characteristics. A theoretical model was applied to explain PL energy-dependency on well width and crystalline orientation taking into account internal electric field for polar substrate. Absence of induced-internal electric field in nonpolar SLs was confirmed by stable PL peak energy and stronger PL intensity as a function of excitation power density than polar ones. © 2010 American Institute of Physics. [doi:10.1063/1.3493185]

The AlGa<sub>x</sub>N/GaN multiquantum-wells (MQWs) and superlattices (SLs) are employed in various device applications such as active regions in UV emitters,<sup>1</sup> cladding layers in visible optical emitters and detectors, gate layers in high mobility transistors,<sup>2</sup> and recently as active layers in intersubband (ISB) devices.<sup>3</sup> These structures are commonly grown along [0001] polar direction. However, due to their noncentrosymmetric and piezoelectric nature, large spontaneous and piezoelectric electric fields are generated along [0001] growth direction. These internal electric fields lead to a substantial quantum confined Stark effect (QCSE) wherein the energy band structure of QWs are bent leading to triangular well potential separating electron and hole wave functions. The QCSE reduces radiative recombination and quantum efficiency and drastically affects optical properties.<sup>4</sup> An efficient approach preventing internal electric fields and consequently QCSE is to employ nonpolar growth directions.

Nonpolar AlGa<sub>x</sub>N/GaN MQWs have been grown on r-plane sapphire<sup>5</sup> and LiAlO<sub>2</sub> (Ref. 6) substrates. However, heteroepitaxial growth on foreign substrates causes lattice-mismatch related strain leading to high density of dislocations and stacking faults at the heterointerfaces. Homoepitaxial growth approach is one of the most effective ways to improve crystalline quality of epilayers. The recent availability of low dislocation density freestanding (FS) c- and m-plane GaN substrates enables studying effects of polarization on optical properties of AlGa<sub>x</sub>N/GaN SLs grown on lattice-matched FS-GaN substrates.<sup>7</sup>

Our recent studies of Al<sub>x</sub>Ga<sub>1-x</sub>N/GaN double barrier resonant tunneling diode demonstrate that low aluminum content ( $x \leq 0.2$ ) active layers improves reliability and reproducibility of ISB devices.<sup>8,9</sup> These are motivating for further studies on low aluminum content AlGa<sub>x</sub>N/GaN SLs. In this paper, we demonstrate high quality regrowth of low aluminum content AlGa<sub>x</sub>N/GaN SLs (employing various well-widths) on polar c-plane and nonpolar m-plane FS-GaN substrates, and correlate the optical properties of these polar and

nonpolar SLs. The substrate orientational dependence of photoluminescence (PL) characteristics is verified with theoretical model.

The growths were carried out in an AIXTRON 200/4-HT horizontal flow low-pressure metal-organic chemical vapor deposition (MOCVD) reactor. Trimethylaluminum and trimethylgallium were used as the metal-organic precursors for Al and Ga, respectively. Ammonia and a mixture of nitrogen and hydrogen gas were used as the anion source and carrier gas, respectively. All SLs have been grown at a pressure of 50 mbar and a growth temperature of 1030 °C. In order to improve the crystalline quality and surface morphology, prior to the growth of the SL structures, a 2 μm thick homoepitaxial GaN layer was grown on the c- or m-plane FS-GaN substrates (Mitsubishi Chemical Co.). The 50 period AlGa<sub>x</sub>N/GaN SL structures, consisting unintentionally doped 4.9 nm thick Al<sub>0.2</sub>Ga<sub>0.8</sub>N barriers and unintentionally doped GaN wells ranging from 1.6 to 6.4 nm in thickness, were grown on c- and m-plane FS-GaN substrates under identical growth conditions.

Structural properties and surface morphologies of the SLs were investigated using open detector omega/2theta x-ray diffraction (XRD) scan [using a Philips high resolution diffractometer system with a monochromator utilizing four (002) Ge reflections] and atomic force microscopy (AFM), respectively. The average aluminum composition of the barriers (that was fixed at 20%) was determined from the angular difference between AlGa<sub>x</sub>N and GaN XRD peaks of bulk AlGa<sub>x</sub>N layers grown on FS-GaN substrates. Thicknesses of SL constituents (barriers and wells) were calibrated as described elsewhere.<sup>10</sup>

Figures 1(a) and 1(b) (left) show omega/2theta (0002) and (10 $\bar{1}$ 0) XRD scans of Al<sub>0.2</sub>Ga<sub>0.8</sub>N(4.9 nm)/GaN(6.4 nm) SLs grown on c- and m-plane FS-GaN substrates, respectively. The simulated XRD diffraction pattern was also appended to Fig. 1. In addition to strong reflections from the GaN substrates, zeroth and first order SL satellite peaks appear for both c- and m-plane. The full-width-at-half-maximum (FWHM) of the zeroth and first order SL peaks for c-plane are 300 arcsec and 107 arcsec and for m-plane are

<sup>a)</sup>Electronic mail: razeghi@eecs.northwestern.edu.

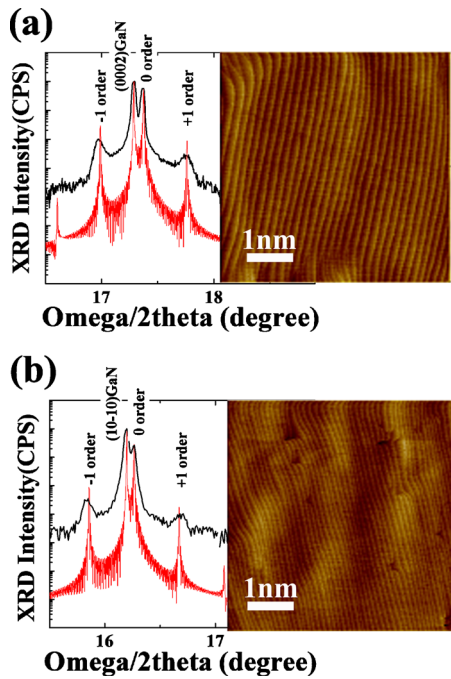


FIG. 1. (Color online) Omega/2theta XRD scan and simulation (left) and ( $5 \times 5 \mu\text{m}^2$ ) AFM image (right) of  $\text{Al}_{0.2}\text{Ga}_{0.8}\text{N}(4.9 \text{ nm})/\text{GaN}(6.4 \text{ nm})$  SL grown on (a) c-plane and (b) m-plane FS-GaN substrates.

391 arcsec and 73 arcsec, respectively, which confirm high crystalline quality as well as high interface quality for both polar and nonpolar SLs. XRD simulations fit well to the observed SL diffraction indicating precise control of barrier Al mole fraction and barrier/well thicknesses. The right part of Figs. 1(a) and 1(b) show  $5 \times 5 \mu\text{m}^2$  AFM images of c- and m-plane SL. Atomically smooth surfaces with very well-aligned atomic steps without any dislocation termination on the surface were achieved for c- and m-plane SL with root mean square (rms) roughnesses of 1.5 Å and 1.3 Å, respectively. These narrow XRD FWHM and low AFM rms roughness values indicate high quality of the SL material growth.

PL measurements for c- and m-plane SLs were performed at room temperature (RT) using frequency double argon-ion laser at 244 nm. Figures 2(a) and 2(b) show PL intensity as a function of energy for c- and m-plane SLs with fixed barrier width (4.9 nm) and different well widths varying from 1.6 to 6.4 nm. The laser excitation power density was fixed at  $11 \text{ W cm}^{-2}$ . Independent of growth direction, as well width increases, a redshift in PL emission energy is observed. This redshift is attributed to reduction in quantum confinement where quantum well width increases and elec-

tron and hole states move toward the bottom of the wells. When well width of c-plane SLs increases over 3.2 nm, emission energy redshifts below the GaN band edge of 3.4 eV (solid line); however, for m-plane SLs, emission energy of SLs approach to GaN band edge energy but never decreases below it. As both c- and m-plane SLs have identical structure (the same barrier Al composition and well and barrier thicknesses), the redshift below the GaN band gap observed in polar SLs is attributed to QCSE due to the internal polarization-induced electric fields leading to triangular well potentials. The quality of polar and nonpolar SLs are also verified by the absence of yellow band emission, which is generally attributed to nitrogen vacancies or impurities.<sup>11</sup> The peak PL spectra of m-plane SLs possess higher intensities and narrower FWHM compared to c-plane SLs indicating higher quality. There is an optimal intensity for each of orientations depending on the well thickness. This optimal intensity can be affected by material quality, interface roughness, excitonic Bohr radius and QCSE, which requires further optical characterization.<sup>5</sup> These results show elimination of internal electric fields by nonpolar substrates leads to more stable and narrower PL emission.

In order to interpret experimental PL results, we performed a simulation that calculates the fundamental transition energy in SLs by solving the Schrödinger equation using the energy-dependent effective mass approximation with a transfer matrix method. The SL is a periodic structure, thus the internal electric fields applied to the GaN wells and Al-GaN barriers depends on the polarization discontinuity, and the well and barrier thicknesses. Therefore, the electric field in the well and the barrier due to spontaneous and piezoelectric polarization along [0001] direction was calculated for polar AlGaIn/GaN SLs according to<sup>12</sup>

$$F_w = b \frac{P_b - P_w}{w\epsilon_b + b\epsilon_w}, \quad (1)$$

$$F_b = -w \frac{P_b - P_w}{w\epsilon_b + b\epsilon_w}, \quad (2)$$

where  $b$ ,  $w$ ,  $\epsilon_b$ , and  $\epsilon_w$  are the barrier and well width, and the barrier and well dielectric constant, respectively.  $P_b$  and  $P_w$  are the total polarization in the barrier and in the well, respectively: the values of  $P_b$  and  $P_w$  have been taken from Ref. 13. The insets of Figs. 2(a) and 2(b) display the experimental and theoretical PL energy of polar c-plane and nonpolar m-plane SLs as a function of well width, respectively. Large separation of electron and hole wave functions induced by internal electric field in c-plane SLs, decreases the

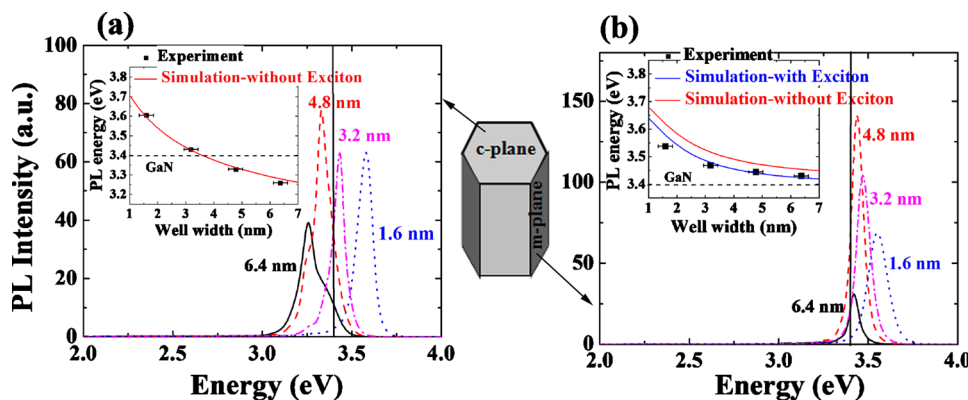


FIG. 2. (Color online) RT PL spectra of the  $\text{Al}_{0.2}\text{Ga}_{0.8}\text{N}(4.9 \text{ nm})/\text{GaN}$  SLs with well widths ranging from 1.6 to 6.4 nm grown on (a) polar c-plane FS-GaN substrates. Inset shows the experimental and simulated PL energy as a function of well width without exciton binding energy effect. (b) Nonpolar m-plane FS-GaN substrate. Inset shows the experimental and simulated PL energy as a function of well width with and without exciton binding energy effect. Solid vertical lines indicate GaN band gap location.

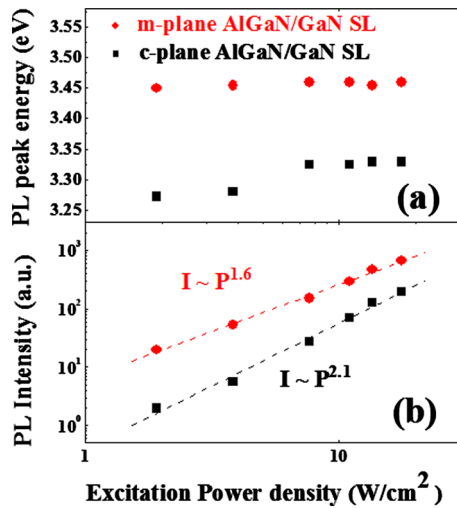


FIG. 3. (Color online) Dependence of (a) the PL peak position and (b) the PL peak intensity on laser excitation power density for  $\text{Al}_{0.2}\text{Ga}_{0.8}\text{N}(4.9 \text{ nm})/\text{GaN}(4.8 \text{ nm})$  SL grown on polar c- and nonpolar m-plane FS-GaN substrates.

exciton binding energy strength. Thus, PL energy was simulated for polar c-plane SLs without taking into account the exciton binding energy effect, which is in good agreement with experiment results. However, for nonpolar m-plane SLs where the internal electric fields are absent, simulations including exciton binding energy effect are in a better agreement with experiential results. The exciton binding energies of GaN/AlGaIn SLs have been taken from Ref. 14. The agreement between theory and experiment confirms that the internal polarization-induced electric fields do not influence the PL emission of nonpolar m-plane SLs, in addition, in the light of simulation, the effect of exciton binding energy in m-plane SLs is observed to be more pronounced than that of c-plane SLs.

Figure 3(a) plots peak PL energy of polar and nonpolar  $\text{Al}_{0.2}\text{Ga}_{0.8}\text{N}(4.9 \text{ nm})/\text{GaN}(4.8 \text{ nm})$  SLs as a function of excitation power density at RT. For the polar c-plane SLs, peaks blueshift by increasing power density (up to  $8 \text{ W}/\text{cm}^2$ ) whereas for nonpolar ones the peak positions are stable. The blueshift of PL peak position in polar SL can be attributed to the polarization-induced electric field whose strength reduces by increasing excitation power due to field screening by carriers<sup>15</sup> and remain unchanged for higher power density ( $8 \text{ W}/\text{cm}^2 <$ ) where carrier screening becomes predominant. Further investigations have been realized via PL excitation power density studies.

Figure 3(b) plots PL intensity as a function of excitation power density for both polar and nonpolar  $\text{Al}_{0.2}\text{Ga}_{0.8}\text{N}(4.9 \text{ nm})/\text{GaN}(4.8 \text{ nm})$  SLs. The PL peak intensity of nonpolar SL is higher than that of polar SL for all excitation power densities. This suggests higher recombination characteristics in nonpolar structures which promise higher quantum efficiency in emitter devices than in polar ones. The intensity ( $I$ ) of PL peaks for a polar SL increases with a 2.1 power index of excitation power density ( $I_{\text{polar}} \sim P^{2.1}$ ), whereas for nonpolar ones it is with a power index of 1.6 ( $I_{\text{nonpolar}} \sim P^{1.6}$ )—in harmony with previous observations.<sup>5,15</sup> This difference in PL intensity power indexes can be explained by strong polarization-induced elec-

tric fields in polar SLs in contrast with nonpolar SLs which decreases electron-hole radiative recombination due to QCSE and reduction in electrons and holes wave functions overlap in triangular wells. Thus, the polar ones have a stronger dependence on the excitation power density than nonpolar ones. Therefore, nonpolar substrates emerge as an attractive substrate for optoelectronic devices with superior performance.

In summary, high quality MOCVD-grown AlGaIn/GaN SLs with various well widths were grown on polar c-plane and nonpolar m-plane FS-GaN substrates and their structural and optical characteristics have been compared. Effects of well width and substrate orientation on structural and optical properties of SLs have been studied using AFM and XRD, and PL studies, respectively. SLs on polar substrate showed strong PL redshift with increasing well width with respect to nonpolar ones. PL power dependent studies showed stable PL peak energy and stronger PL intensity for nonpolar m-plane SLs than polar ones indicating absence of induced electric fields and consequent QCSE in m-plane SLs. A theoretical model was applied to explain the PL energy dependencies on SLs design and substrate orientation. Our results demonstrate that m-plane FS-GaN substrates are promising candidates for optoelectronic devices thanks to the improved recombination characteristics and stability of wavelength emission.

The authors acknowledge Dr. J. Zavada of ARO, Dr. J. Mangano, and Dr. Scott Rodgers of DARPA, and Mr. Jerry Speer of U.S. Army RDECOM for their interest and encouragement, and Mr. Bayram acknowledges IBM and Link Foundation Energy Fellowships.

<sup>1</sup>H. Yoshida, Y. Takagi, M. Kuwabara, H. Amano, and H. Kan, *Jpn. J. Appl. Phys., Part 1* **46**, 5782 (2007).

<sup>2</sup>K. H. Lee, P. C. Chang, S. J. Chang, Y. K. Su, and C. L. Yu, *Appl. Phys. Lett.* **96**, 212105 (2010).

<sup>3</sup>N. Péré-Laperne, C. Bayram, L. Nguyen-Thê, R. McClintock, and M. Razeghi, *Appl. Phys. Lett.* **95**, 131109 (2009).

<sup>4</sup>D. Queren, A. Avramescu, G. Brüderl, A. Breidenassel, M. Schillgalies, S. Lutgen, and U. Strau, *Appl. Phys. Lett.* **94**, 081119 (2009).

<sup>5</sup>M. D. Craven, P. Waltereit, J. S. Speck, and S. P. DenBaars, *Appl. Phys. Lett.* **84**, 496 (2004).

<sup>6</sup>P. Waltereit, O. Brandt, A. Trampert, H. T. Grahn, J. Menniger, M. Ramsteiner, M. Reiche, and K. H. Ploog, *Nature (London)* **406**, 865 (2000).

<sup>7</sup>Z. Vashaei, E. Cicek, C. Bayram, R. McClintock, and M. Razeghi, *Appl. Phys. Lett.* **96**, 201908 (2010).

<sup>8</sup>C. Bayram, Z. Vashaei, and M. Razeghi, "Reliability in room temperature negative differential characteristics of low-aluminium-content AlGaIn/GaN double-barrier resonant tunneling diodes," *Appl. Phys. Lett.* (unpublished).

<sup>9</sup>C. Bayram, Z. Vashaei, and M. Razeghi, *Appl. Phys. Lett.* **97**, 092104 (2010).

<sup>10</sup>Z. Vashaei, C. Bayram, and M. Razeghi, *J. Appl. Phys.* **107**, 083505 (2010).

<sup>11</sup>L. Polenta, A. Castaldini, and A. Cavallini, *J. Appl. Phys.* **102**, 063702 (2007).

<sup>12</sup>F. Bernardini and V. Fiorentini, *Phys. Status Solidi B* **216**, 391 (1999).

<sup>13</sup>O. Ambacher, J. Majewski, C. Miskys, A. Link, M. Hermann, M. Eickhoff, M. Stutzmann, F. Bernardini, V. Fiorentini, V. Tilak, B. Schaff, and L. F. Eastman, *J. Phys.: Condens. Matter* **14**, 3399 (2002).

<sup>14</sup>T. Y. Chung and K. J. Chang, *Semicond. Sci. Technol.* **13**, 876 (1998).

<sup>15</sup>E. Kuokstis, C. Q. Chen, M. E. Gaevski, W. H. Sun, J. W. Yang, G. Simin, M. Asif Khan, H. P. Maruska, D. W. Hill, M. C. Chou, J. J. Gallagher, and B. Chai, *Appl. Phys. Lett.* **81**, 4130 (2002).